Plasmonic materials based on ZnO films and their potential for developing broadband middle-infrared absorbers

Yunus E. Kesim, Enes Battal, and Ali K. Okyay

Articles you may be interested in

ZnO plasmonics for telecommunications
Appl. Phys. Lett. **102**, 182107 (2013); 10.1063/1.4804984

Optimization of Al-doped ZnO films for low loss plasmonic materials at telecommunication wavelengths
Appl. Phys. Lett. **102**, 171103 (2013); 10.1063/1.4802901

Optical transmission properties of perforated metal films in the middle-infrared range
Appl. Phys. Lett. **94**, 081118 (2009); 10.1063/1.3088858

Middle-infrared transmission enhancement through periodically perforated metal films
Appl. Phys. Lett. **84**, 2977 (2004); 10.1063/1.1711166

Development of interfacial microstructure during cooling of a ZnO varistor material
J. Appl. Phys. **66**, 5072 (1989); 10.1063/1.343783

Plasmonic materials based on ZnO films and their potential for developing broadband middle-infrared absorbers

Yunus E. Kesim,[1,2,a] Enes Battal,[1,2] and Ali K. Okyay[1,2,3]
[1]*Department of Electrical and Electronics Engineering, Bilkent University, Ankara, 06800, Turkey*
[2]*UNAM-National Nanotechnology Research Center, Bilkent University, Ankara, 06800, Turkey*
[3]*Institute of Materials Science and Nanotechnology, Bilkent University, Ankara, 06800, Turkey*

Noble metals such as gold and silver have been extensively used for plasmonic applications due to their ability to support plasmons, yet they suffer from high intrinsic losses. Alternative plasmonic materials that offer low loss and tunability are desired for a new generation of efficient and agile devices. In this paper, atomic layer deposition (ALD) grown ZnO is investigated as a candidate material for plasmonic applications. Optical constants of ZnO are investigated along with figures of merit pertaining to plasmonic waveguides. We show that ZnO can alleviate the trade-off between propagation length and mode confinement width owing to tunable dielectric properties. In order to demonstrate plasmonic resonances, we simulate a grating structure and computationally demonstrate an ultra-wide-band (4–15 μm) infrared absorber. © 2014 Author(s). All article content, except where otherwise noted, is licensed under a Creative Commons Attribution 3.0 Unported License. [http://dx.doi.org/10.1063/1.4887520]

I. INTRODUCTION

Plasmonics is touted as a milestone in optoelectronics[1] as this technology can form a bridge between electronics and photonics, enabling the integration of electronics and photonic circuits at the nanoscale.[2] The leading paper by Ebbesen et. al. in 1998[3] encouraged studies in this area and today applications of plasmonics span a wide range including sub-wavelength waveguiding,[4] imaging[5] and lithography;[6] optical interconnects[7] and photonic circuits;[8] chemical/biological sensors;[9,10] improved photovoltaic devices[11,12] such as perfect absorbers.[13,14]

Although noble metals such as gold and silver are widely used in plasmonic applications, there is a significant drawback associated with such metals: high optical loss. Recently, there is an increased effort in the search for alternative plasmonic materials including Si, Ge, III-Nitrides and transparent conductive oxides.[15–19] The main appeal of these materials, most of them semiconductors, is their lower optical losses, especially in the infrared (IR) regime, compared to noble metals owing to their lower number of free electrons.[15–19] Other advantages can be listed as low-cost and control on plasma frequency thanks to the tunable electron concentration i.e. effective doping level.[15]

Several research groups demonstrated transparent conductive oxides such as Al:ZnO, Ga:ZnO and indium-tin-oxide (ITO) as potential plasmonic materials.[15–19] In this paper, we computationally demonstrate an ultra-wide-band (4–15 μm) infrared plasmonic absorber based on atomic layer deposition (ALD) grown ZnO. ALD grown ZnO is known to have crystal imperfections such as O vacancies that behave as n-type dopants.[20,21] An advantange of ALD grown ZnO is the viability of tuning carrier concentration by the growth temperature. As the growth temperature increases, number of O vacancies increases which results in higher carrier concentration.

---

[a]Author to whom correspondence should be addressed: Electronic mail: yunus.kesim@bilkent.edu.tr
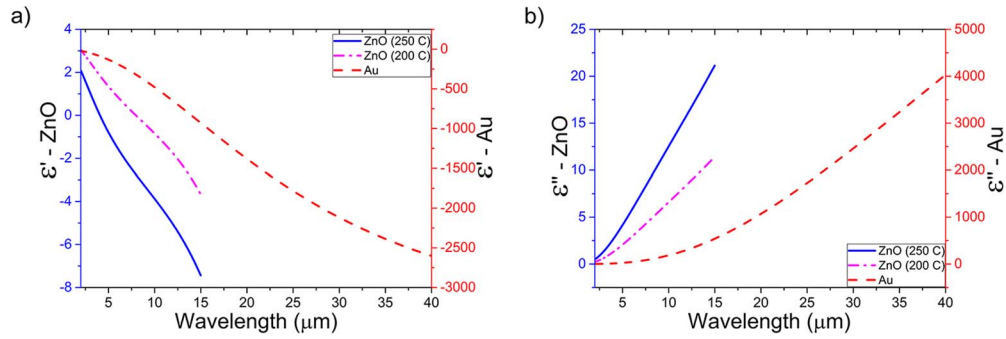
4, 077106-1

FIG. 1. a) Real and b) imaginary parts of dielectric permittivity of Au (see Ref. 22) and ZnO grown at 200 ºC and 250 ºC.

A grating array is chosen as the proof-of-concept plasmonic scheme. With a careful design, more than 70% average absorption is achieved throughout the 4–15 μm wavelength regime, with a film thickness of less than 2.5 μm. Furthermore, $\sim$90% of incident light is absorbed in the all-important 8–12 μm wavelength regime, referred to as the long-wave IR (LWIR) band for IR imaging applications.

II. MATERIALS CHARACTERIZATION

The high optical losses associated with metals in the IR regime is attributed to the Drude response of high number of free electrons which is given by

$$\epsilon = \epsilon' + j\epsilon'' = \epsilon_\infty + \frac{\omega_p^2}{\omega^2 + \gamma^2} + j\frac{\omega_p^2}{(\omega^2 + \gamma^2)\omega} \tag{1}$$

where ϵ_∞ is the background permittivity, ω_p is the plasma frequency and γ is the damping factor. For low optical loss, imaginary part of the permittivity is required to be small. Therefore, plasma frequency, ω_p, which is proportional to electron concentration, is the key factor that determines the loss. For noble metals, electron concentration is on the order of 10^{22} per cubic centimeter. The advantage of using ZnO as a plasmonic material arises from the ability of modern growth technologies to tune carrier concentration.

ALD growth of ZnO is carried out using a Cambridge Savannah 100 Thermal ALD system using diethylzinc (DEZ) and milli-Q water (H_2O) as precursors on n-type (100) Si wafers. The growth is conducted at 200 ºC and 250 ºC. Without any further annealing, ellipsometric characterization of as-grown films are conducted using J.A. Woollam V-Vase (0.4–1.7μm) and IR-Vase (1.8–15μm) ellipsometers. The permittivity values of ZnO films are graphed on Figure 1, alongside with the permittivity of Au for comparison.[22]

Real part of dielectric permittivity of ZnO grown at 250 ºC is equal to 0 at a wavelength of 4.08 μm. Corresponding plasma frequency is $\omega_p = 4.62 \times 10^{14}$ rad/s. Plasma frequency can also be determined using the following expression:

$$\omega_p^2 = \frac{Nq^2}{\epsilon_o m^*} \tag{2}$$

where N is electron density, q is electronic charge, ϵ_o is vacuum permittivity and m^* is effective electron mass for ZnO. Substituting $m^* = 0.23m_o$ where m_o is the electron mass,[23] carrier density of the ZnO film can be found as $N = 1.542 \times 10^{19}$ cm^{-3}. This carrier density is sufficiently close to the reported values in the literature.[24] The slight difference can be attributed to different growth conditions. Similarly, electron density of the ZnO film grown at 200 ºC can be found as 4.056 $\times 10^{18}$ cm^{-3}.

We also investigate the propagation length (L_P) and confinement width (D_W) of surface plasmons propagating at the ZnO/air interface and compare with that at Au/air interface.[25] These quantities
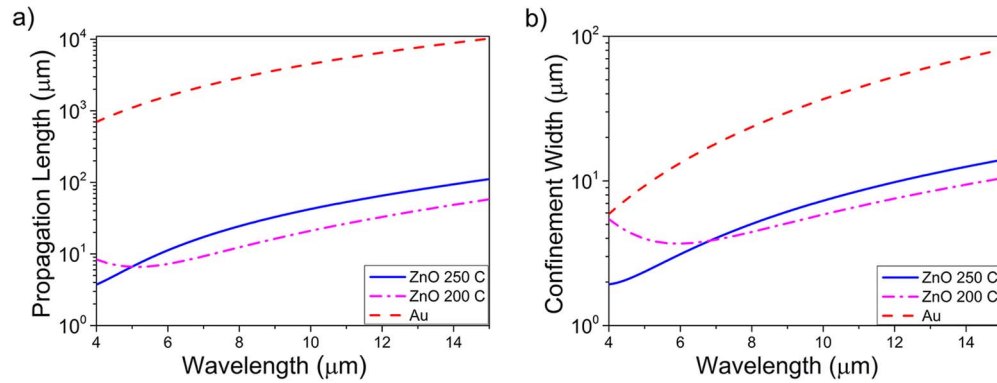
FIG. 2. Comparison of Au and ZnO grown at 200 ºC and 250 ºC in terms of **a)** surface plasmon propagation length and **b)** mode confinement width at air interface. Gold offers higher propagation length, yet ZnO provides higher confinement of the electromagnetic field. Also, ZnO allows to fine tune these figures as there is a nuance between the performances of ZnO grown at 200 ºC and 250 ºC.

are a measure of performance for plasmonic waveguide applications and can be calculated using

$$L_P = 1/Im \left\{ k_o \sqrt{\frac{\epsilon_m}{1 + \epsilon_m}} \right\} \tag{3}$$

$$D_W = \begin{cases} \delta_{air}, & |\varepsilon_m| \geq e \\ \delta_{air} + \delta_m(1 - \ln(|\varepsilon_m|)), & |\varepsilon_m| < e \end{cases} \tag{4}$$

where ϵ_m is the permittivity of the plasmonic material; $\delta_{air} = 1/Re \left\{ k_o \sqrt{-1/(\epsilon_m + 1)} \right\}$ and $\delta_m = 1/Re \left\{ k_o \sqrt{-\epsilon_m^2/(1 + \epsilon_m)} \right\}$ are the penetration depths in air and plasmonic material, respectively. On Figure 2, the propagation length and the confinement width for air/ZnO interface and air/Au interface are compared. In surface plasmon waveguides, there is a trade-off between the propagation length and the confinement width[25] and it is clearly seen in Figure 2 below. While Au enjoys a longer propagation length, ZnO films allow a better confinement of the field. Therefore, while choosing a material, one should balance this trade-off between propagation length and the confinement width. Since the optical parameters can be easily tuned by changing the growth temperature, ZnO gives a higher degree of freedom by offering control of the parameters that determine the figure of merit and allow their effective optimization.

III. INFRARED ABSORBER STRUCTURE

As proof of concept, a grating structure (Figure 3) is simulated using finite-difference time-domain method using *FDTD Solutions* of *Lumerical Inc*. For grating coupling, phase matching condition is fulfilled when

$$k_{sp} = k_0 sin\theta + mG \tag{5}$$

is satisfied where k_{sp} and k_0 are wavevectors of plasmons and the incident light in free space, respectively; G is the reciprocal vector of the grating structure and m is an integer. For normal incident light, $\theta = 0$ and for the first order resonance $m = 1$. Substituting the expression for plasmon wavevector and G in terms of wavelength and period of the grating, the resonant wavelength of the air/ZnO interface can be found as

$$\lambda \cong P \sqrt{\frac{\epsilon}{1 + \epsilon}} \tag{6}$$

where P is the center to center distance of the gratings, i.e. the period and ε is the dielectric constant of ZnO. For $\epsilon \gg 1$, $\lambda \approx P$.
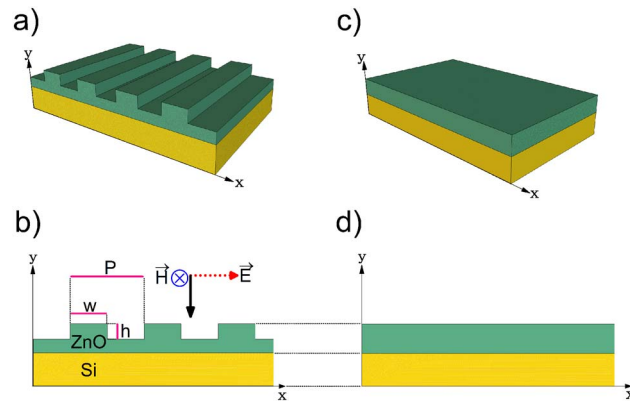
FIG. 3. Simulated structures: Plasmonic grating structure, **a)** 3D and **b)** 2D side view. TM polarized EM wave has electric field along x axis. Reference structure, **c)** 3D and **d)** 2D side view. Note that, the thickness of ZnO film is same for the reference and the grating structure.

A 2-D simulation setup is configured with the periodic boundary conditions on the x axis and perfectly matched layers on the y axis. The structure is illuminated with a plane wave source where the wavelength range of the light is 4–15 μm. Also, the plane wave is TM polarized, i.e. the electric field is along the x axis, which enables the generation of surface plasmons in the grating structure. The mesh grid around and inside ZnO region is set such that the mesh steps in x and y directions are 25 nm. Si is chosen as substrate since it is common and modelled with a constant refractive index n = 3.42 and extinction coefficient k = 0, within the wavelength range of interest. The ZnO film is modelled using the optical parameters of ZnO grown at 250 ℃.

For demonstration purpose, the period is chosen $P = 5$ μm, width of the grating is chosen as $w = 4$ μm and the grating height is $h = 1.5$ μm. The base thickness of ZnO is chosen as 1 μm, in order to de-couple the resonances in the gratings from the effects of the substrate, as we are aiming to generate plasmons at the air/ZnO interface. In order to investigate resonant conditions, absorption in the ZnO film is calculated using the difference of power transmission through two field monitors, one located on top of gratings (y = 2.5 μm) and one at the ZnO/Si interface (y = 0). The power transmission through the top monitor at y = 2.5 μm is $P_1 = 1 - R$, where 1 denotes the incident light and R is the reflection from the grating structure. The transmission through the monitor at y = 0 is $P_2 = T$ where T is the power transmitted through the ZnO film. The absorbed power (A) can be calculated using A = 1 − R − T which equals A = $P_1 - P_2$.

Also, for comparison, a reference simulation setup is formed where a slab of ZnO which does not utilize gratings is placed on Si substrate (Figures 3(c) and 3(d)). The thickness of the ZnO slab is 2.5 μm and the absorption is calculated similar to the plasmonic structure.

The absorption spectra for both of the structures are given on Figure 4(a). A resonance peak is observed at a wavelength that is very close to the grating periodicity of 5 μm. This resonace can be attributed to the excitation of surface plasmon polaritons as described by the equation given in (6).[26] For $\epsilon \gg 1$, the equation reduces to $\lambda \approx P$ (for ZnO, $\varepsilon = -0.797 + j4.162$ at $\lambda = 5$ μm). In addition, a stronger broadband resonance is observed at 11.5 μm. Since the separation between the gratings are much lower than the grating width, the structure can be treated as a truncated MDM slot waveguide and supports a fundamental edge mode.[27,28] In Figure 4(b) (multimedia view), the intensity profile at $\lambda = 11.5$ μm is given and field intensity is maximum at the edges. This can be attributed to the singular behavior of electric field near sharp edges. That the field intensity is 0 in the base ZnO and the Si substrate shows that the incident light is not coupled into the substrate layer through the grating waveguide effect.[29,30]

Finally a parameter sweep is conducted in order to investigate the structural dependence of the absorption spectra (Figure 5). When $P = 5$ μm, there is a resonance at 5 μm as expected and when $P = 4.4$ μm, the resonance shifts to 4.4 μm. Figure 5 shows that the wavelength of the broadband
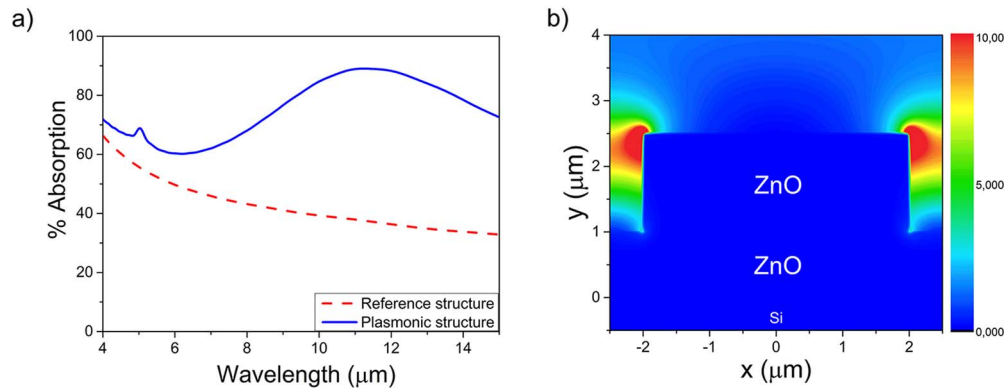
FIG. 4. a) Comparison of the absorption spectra of the reference structure and the plasmonic structure. **b)** Electric field intensity profile around the gratings ($\lambda = 11.5\ \mu$m) (multimedia view). [URL: http://dx.doi.org/10.1063/1.4887520.1]
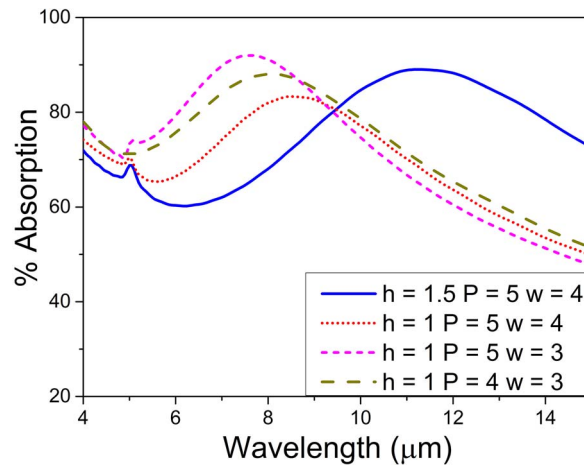

FIG. 5. Absorption spectra for different structures. As other plasmonic devices demonstrated using conventional metals,[13] ZnO absorber allows the spectra to be tuned.

resonance is affected both by w and h. The grating width (w) determines the plasmon wavevector along the slot waveguide[31] and the height of the grating affects the supported mode.[28]

Recently, our group demonstrated ZnO as a possible candidate for the absorber material in microbolometers that are used for infrared imaging.[32] In Figure 4, the significant contribution of plasmons to the absorption spectra is clear. Also, Figure 5 shows that the resonances can be tuned. Therefore, the structure can be tailored to achieve maximum absorption in a desired spectral range. An optimum design is sought in order to maximize the average absorption in 4–15 μm band. The period of the structure is varied from 1 μm to 5 μm, and the height of the gratings are swept from 0.5 μm nm to 1.5 μm. For each of these two parameters, the width of the gratings is also varied where the minimum width is 100 nm and the maximum width is the 80% of the corresponding period. The base thickness of ZnO was kept constant, i.e. 1 μm. For each structure, reference structures are also created where a slab of flat ZnO that has the same thickness is placed on Si substrate. For both sets of structures absorption in the 4–15 μm band are calculated. When the grating has a height of 1.4 μm, a period of 1.8 μm and a width of 1.2 μm; the absorption is maximized. The absorption spectra of this structure is given on Figure 6. For the entire spectrum, absorption is over 70% and the average absorption in this spectrum is $\sim$ 85%.

The design shown in Figure 6 also provides maximum absorption in the 8–12 μm range which is the popular long-wave infrared (LWIR) atmospheric transmission window that is used commonly for thermal imaging. Average absorption in this range is $\sim$ 93% and it is $\sim$ 2.34 folds higher than
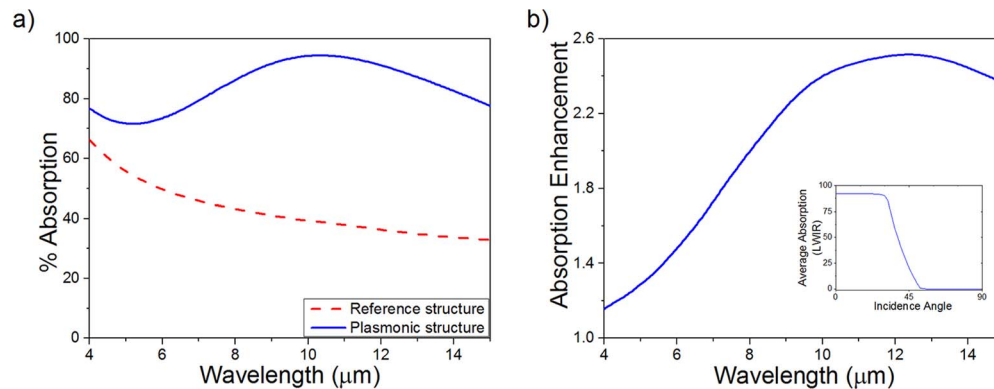
FIG. 6. a) Comparison of the absorption spectra of the reference structure and the plasmonic structure when $P = 1.8$ μm, $w = 1.2$ μm and $h = 1.4$ μm. **b)** Absorption enhancement is the ratio of % absorption of plasmonic structure to the % absorption of the reference structure. Inset shows how the average absorption of the plasmonic structure in the LWIR band changes when the incidence angle is changed.

the absorption of the reference structure. Also, we conducted simulations where the angle of the incident light is changed from $0°$ (normal incidence) to $90°$ and calculated average absorption in the LWIR band. Up to $30°$, the structure still shows high absorption characteristics, then starts to drop and reaches near 0 absorption at around $50°$ (Figure 6(b), inset).

IV. CONCLUSION

In conclusion, we have introduced ALD grown ZnO as an alternative plasmonic material in the infrared. The dielectric permittivity values of ZnO grown at different temperatures are extracted and we have shown that the plasma frequency of ALD grown ZnO depends on growth temperature. The ability to tune the optical properties enables effective optimization of propagation loss and mode confinement width of plasmonic devices. Furthermore, we simulated a plasmonic grating coupler and demonstrated plasmonic resonances at the ZnO/air interface. The absorption spectrum of the simulated device show exceptional performance enhancement over reference device in the 4–15 μm wavelength band. We also demonstrated that, with an optimization of structural parameters, such an absorber can be used in microbolometers for infrared imaging in the 8–12 μm band.

[1] D. Pile, Nature Materials **9**, S18 (2010).
[2] E. Ozbay, Science **311**, 189 (2006).
[3] T. W. Ebbesen, H. J. Lezec, H. F. Ghaemi, T. Thio, and P. A. Wolff, Nature **391**, 667 (1998).
[4] D. F. P. Pile and D. K. Gramotnev, Opt. Lett. **30**, 1186 (2005).
[5] S. Kawata, Y. Inouye, and P. Verma, Nat. Photonics **3**, 388 (2009).
[6] W. Srituravanich, N. Fang, C. Sun, Qi Luo, and X. Zhang, Nano Lett. **4**, 1085 (2004).
[7] E. Battal and A. K. Okyay, Opt. Lett. **38**, 983 (2013).
[8] S-W Qu and Z-P Nie, Sci. Reports **3**, 3172 (2013)
[9] K. Chen, R. Adato, and H. Altug, ACS Nano **6**, 7998 (2012).
[10] R. Adato, A. A. Yanik, J. J. Amsden, D. L. Kaplan, F. G. Omenetto, M. K. Hong, S. Erramili, and H. Altug, Proc. Natl. Acad. Sci. **106**, 19227 (2009).
[11] H. A. Atwater and A. Polman, Nat. Mater. **9**, 205 (2010).
[12] F. B. Atar, E. Battal, L. E. Aygun, B. Daglar, M. Bayindir, and A. K. Okyay, Opt. Express **21**, 7196 (2013).
[13] M. Pu, C. Hu, M. Wang, C. Huang, Z. Zhao, C. Wang, Q. Feng, and X. Luo, Opt. Express **19**, 17413 (2011).
[14] J. Hao, L. Zhou, and M. Qiu, Phys. Rev. B **83**, 165107 (2011).
[15] G. V. Naik, V. M. Shalaev, and A. Boltasseva, Adv. Mater. **25**, 3264 (2013).

[16] S. Q. Li, P. Guo, L. Zhang, W. Zhou, T. W. Odom, T. Seideman, J. B. Ketterson, and R. P. H. Chang, ACS Nano **5**, 9161 (2011).

[17] G. V. Naik, J. Kim, and A. Boltasseva, Opt. Mater. Express **1**, 1090 (2011).

[18] J. Kim, G. V. Naik, N. K. Emani, U. Guler, and A. Boltasseva, IEEE J. Select. Topics Quantum Electron. **19**, 4601907 (2013).

[19] G. V. Naik, J. Liu, A. V. Kildishev, V. M. Shalaev, and A. Boltasseva, Proc. Natl. Acad. Sci. **109**, 8834 (2012).

[20] L. E. Aygun, F. B. Oruc, F. B. Atar, and A. K. Okyay, IEEE Photonics Journal **5**, 2200707 (2013).

[21] S. Alkis, B. Tekcan, A. Nayfeh, and A. K. Okyay, J. Opt. **15**, 205002 (2013).

[22] R. L. Olmon, B. Slovick, T. W. Johnson, D. Shelton, S.-H. Oh, G. D. Boreman, and M. B. Raschke, Phys. Rev. B **86**, 235147 (2012).

[23] W. R. L. Lambrecht, A. V. Rodina, S. Limpijumnong, B. Segall, and B. K. Meyer, Phys. Rev. B **65**, 075207 (2002).

[24] E. Guziewicz, M. Godlewski, L. Wachnicki, T. A. Krajewski, G. Luka, S. Gieraltowska, R. Jakiela, A. Stonert, W. Lisowski, M. Krawczyk, J. W. Sobczak, and A. Jablonski, Semicond. Sci. Technol. **27**, 074011 (2012).

[25] P. Berini, Opt. Express **14**, 13030 (2006).

[26] F. J. Garcia de Abajo, J. J. Saenz, I. Campillo, and J. S. Dolado, Opt Express **14**, 7 (2006).

[27] G. Veronis and S. Fan, J. Lightw. Technol. **25**, 2511 (2007).

[28] M. Bora, B. J. Fasenfest, E. M. Behymer, A. S-P. Chang, H. T. Nguyen, J. A. Britten, C. C. Larson, J. W. Chan, R. R. Miles, and T. C. Bond, Nano Lett. **10**, 2832 (2010).

[29] Y. Chen, Z. Zhang, and M. Yu, Appl. Phys. Lett. **103**, 061109 (2013).

[30] D. Rosenblatt, A. Sharon, and A. A. Friesem, IEEE J. Quant. Electr. **33**, 2038 (1997).

[31] J. A. Dionne, L. A. Sweatlock, and H. A. Atwater, Phys. Rev. B **73**, 035407 (2006).

[32] E. Battal, S. Bolat, M. Y. Tanrikulu, A. K. Okyay, and T. Akin, "Atomic Layer Deposited Zinc-Oxide as Tunable Uncooled Infrared Microbolometer Material" Physica Status Solidi A.